Bulletin of Electrical Engineering and Informatics
Vol. 14, No. 6, December 2025, pp. 4174~4188
ISSN: 2302-9285, DOI: 10.11591/eei.v14i6.11044

Parameter tuning of PIDG controller on maximum photovoltaic power point for battery charging system

Muhammad Irwanto[1,2], Togar Timoteus Gultom[1], Habib Satria[3], Baharuddin Ismail[2], Christin Erniati Panjaitan[1], Mahdi Syukri[4]

[1]Center of Excellence for Health Based on IoT and Renewable Energy, Department of Electrical Engineering, Faculty of Science and Technology, Universitas Prima Indonesia (UNPRI), Medan, Indonesia
[2]Fellow of Center of Excellence for Renewable Energy (CERE), Faculty of Electrical Engineering and Technology, Universiti Malaysia Perlis (UniMAP), Perlis, Malaysia
[3]Department of Electrical Engineering, Faculty of Technology, Universitas Medan Area (UMA), Medan, Indonesia
[4]Department of Electrical and Computer Engineering, Faculty of Technology, Universitas Syiah Kuala (USK), Banda Aceh, Indonesia

Article Info

Article history:

Received Jul 16, 2025
Revised Sep 10, 2025
Accepted Sep 27, 2025

Keywords:

Battery charging system
DC-DC buck converter
Maximum photovoltaic power
Parameter tuning
Photovoltaic module
Proportional integral derivative controller
Proportional integral derivative with gain controller

ABSTRACT

Maximum photovoltaic power point (MPVPP) based on DC-DC buck converter is supplied by photovoltaic module. A controller method is needed to control the signal that it drives the switching component of DC-DC buck converter. The previous researcher conducts proportional integral derivative (PID) controller applying the DC-DC buck converter, but only its parameters (proportional, K_P, integral, K_I, and derivative, K_D) are studied. This paper presents MPVPP based on PID with gain (PIDG) controller on the DC-DC buck converter by tuning the parameters of K_P. K_I and K_D and adding a gain, G connected to PIDG controller for charging 12 V, 7 Ah battery. The DC-DC buck converter is designed for the output voltage of 14.7 V and output power of 150 W and modelled using Simulink MATLAB. The simulation results show that the parameters of K_P=0.0032, K_I=1, and K_D=4×10^{-7} are suitable to control the switching component. The gain, G gives significant effect on the settling time and the time to reach their steady state value of output voltage of 14.7 V. The battery SOC can increase 1.36% per second, if the initial SOC is 25%, thus it needs arround 55 seconds to reach the fully charging condition.

Corresponding Author:

Muhammad Irwanto
Center of Excellence for Health Based on IoT and Renewable Energy
Department of Electrical Engineering, Faculty of Science and Technology
Universitas Prima Indonesia (UNPRI)
Medan, Indonesia
Email: muhammadirwanto@unprimdn.ac.id

1. INTRODUCTION

An electrical device that can convert solar energy into electrical energy is a photovoltaic (PV) module. 95% of the PV module industry is made up of silicon (Si) material, which is crucial to their manufacture [1], [2]. These days, PV module construction technology is advancing quickly, lowering carbon emissions and replacing less ecologically friendly conventional energy [3]. Temperature affects how a PV module operates; a typical temperature of 25 °C is needed to reach the maximum power, open circuit voltage, and short circuit current [4]. Mathews *et al.* [5] examines how solar radiation conditions impact PV module output power; specifically, for Cadmium Telluride (CdTe) PV modules, higher solar radiation results in higher PV module output power, whereas lower solar radiation results in lower PV module output power.

Using an inverter, the PV module can be utilized in AC load applications, as demonstrated in the standalone system by [6], which uses HOMER to compare and analyze the technical and economic aspects of the various tilt angles of PV modules. Zaghba *et al.* [7] also uses Simulink MATLAB to simulate a standalone PV system, which consists of a 2 kW PV module coupled to an inverter and battery to supply AC loads. A battery operation controller is built into this system to regulate the energy supply from the battery or PV module.

PV modules can apply DC loads either directly or through the use of a DC-DC converter. A DC voltage source is converted by the DC-DC converter to a DC output voltage that is either higher or lower than the input voltage [8]. DC-DC buck converter, DC-DC boost converter, and DC-DC buck boost converter are among the different kinds of DC-DC converters [9]–[13]. The DC voltage source is changed from a higher voltage level to a lower output voltage level via the DC-DC buck converter. The DC voltage source is converted from a lower voltage level to a greater output voltage level by the DC-DC boost converter [14], [15]. The DC-DC buck boost converter, on the other hand, is a hybrid of a buck and a boost converter. It can function as either a buck converter or a boost converter depending on its operating duty cycle.

A diode, an inductor, a capacitor, a resistor, and a switching component (metal–oxide–semiconductor field–effect transistor (MOSFET), insulated gate bipolar transistor (IGBT), or transistor) make up the DC-DC buck converter [16]–[18]. The maximum PV power point (MPVPP), which is the maximum output power of a PV module, can be tracked using a DC-DC buck converter. Stable output performance of the DC-DC buck converter depends on a controller mechanism that regulates the pulse–width modulation (PWM) sign in the switching components. It has been modified to meet the requirements of DC load applications.

Electrical control systems have made extensive use of proportional integral derivative (PID) controllers. The PID controller was created by several academics in order to improve controller performance in electrical applications. Rajesh and Deepa [19] designed a PID controller with a double derivative, known as a PIDD controller enhanced by reference adaptive control (RAC) model. Using the particle swarm optimization (PSO) method, the PIDD controller's parameters are adjusted to regulate the servo motor's speed. To regulate the switching reluctance motor, the same researcher [20] uses the flower pollination method. It is used to increase the motor's dynamic performance and smooth torque stability.

Rajesh and Deepa [21] also examines the use of the PSO algorithm to adjust the PID controller's ideal values. The linear quadratic regulator (LQR) completes the PID controller in this system, which is known as the fractional order PID (FOPID) controller. It uses pole placement for feedback in order to stabilize the inverted pendulum model's performance. Rajesh [22] applies additional FOPID controller research to the single conical tank system. The FOPID controller's parameters are adjusted using the PSO technique. It is used to regulate the tank's internal liquid level. It is utilized in tank system hardware. In comparison to other conventional controllers, the FOPID controller's results on the tanks system demonstrate its smooth reaction and good performance in controlling the liquid level.

Research by [23]–[27] use the perturb and observe (P&O) algorithm to manage the PWM signal on the DC-DC boost converter. Stabilizing the DC-DC boost converter's output performance is the primary goal of this approach. This algorithm is dependent on the PV module's output voltage and current. In order to make a choice, the algorithm multiplies the PV module's output power by its output voltage and current. Three output power selections are used to manage the system: the output power is less than zero, equals zero, and exceeds zero.

For the DC-DC converter, Ouyang *et al.* [28] suggests a controller method utilizing fuzzy proportional integral (PI) controller. The fuzzy controller receives two input signals from the sum of the reference voltage, the DC-DC converter's output voltage, and its derivative. The fuzzy PI controller method generates two signals, which are then used to adjust the PI controller's two parameters (integral, K_I and proportional, K_p). The fuzzy PI controller does not employ a derivative controller, nor does it add gain or G either before or after the controller system. On the DC-DC buck converter, Samosir *et al.* [29] also applies a PID controller using a straightforward technique to adjust its settings (proportional, K_p, integral, K_I, and derivative, K_D). Additionally, the gain, G, is not applied prior to or following the controller system.

This paper presents a parameter tuning and a gain, G on the MPVPP for battery charging system. The MPVPP is constructed by DC-DC buck converter based on PIDG controller. The electrical parameters of DC-DC buck converter (inductor, L, capacitor, C, and resistor, R) are calculated to obtain its required output voltage and power. The parameters of PIDG controller (proportional, K_p, integral, K_I, and derivative, K_D) are also tuned to stable its steady state output voltage. A gain, G is applied after PID controller to obtain the shortest settling time and the shortest time to achieve its steady state output voltage. The performances of PV module, DC-DC buck converter and battery are observed and analyzed under standard test condition and various solar irradiance. Also, the effect of gain, G on the performance of DC-DC buck converter is analyzed.

Future works of this research are in the implementation of artificial intelligent method (such as genetic algorithm, fire fly algorithm, machine learning, and fuzzy logic) for finding the parameters of PIDG controller. Hardware of MPVPP system can be implemented by using Arduino Uno or PIC microcontroller for tuning the

PIDG controller. The oscillation of output voltage of DC-DC buck converter can be observed using oscilloscope to know the system stability. Also, the thermal effect on the DC-DC buck converter and battery can be study further.

2. METHOD

The DC-DC buck converter design, PIDG controller parameter tuning, battery charging, and the PV modul as a DC voltage source in the system as a whole are all explained in this part. The purpose of the DC-DC buck converter is to lower the PV module's voltage to the level needed for the battery charging system. The transfer function concept is used to adjust the PIDG controller's parameters (proportional, K_P, integral, K_I, and derivative, K_D) with its different gains in order to get the DC-DC buck converter's steady state values in the shortest amount of time. The PV module is used throughout the DC-DC buck converter to charge a 12 V battery.

2.1. Modelling of photovoltaic module as DC voltage source in the system

The Shinyoku PV module is used in PV module modeling, with its electrical properties displayed in Table 1 [30]. Maximum power, open circuit voltage, and short circuit current are the primary electrical parameters. Two solar irradiance settings are used to characterize the PV module: the first is 1000 W/m^2 of solar irradiance and 25 °C (standard test conditions); the second is a constant temperature of 25 °C with different solar irradiance. The primary goal is to see how well the DC-DC buck converter performs under these circumstances.

Table 1. The electrical parameters of Shinyoku PV module

Parameters	Value
Open circuit voltage	20.64 V
Maximum power	20 W
Short circuit current	1.3 A
Open circuit voltage at the maximum power	17.2 V
Short circuit current at the maximum power	1.16 A
Temperature coefficient at the open circuit voltage	-0.15%/ ºC
Temperature coefficient at the short circuit current	0.15%/ ºC

Figure 1 illustrates how Simulink MATLAB is used to model the PV module. The PV module's block parameters are filled in using the values found in Table 1. To reach the output voltage of 20.64 V on the regulated voltage source connected to the DC-DC buck converter's input terminal, a resistance of 48 Ω is connected in parallel. Based on the standard test conditions (STC) condition, the PV module's performance is monitored, examined, and verified. The error percentage that is a comparison between the electrical parameters and the simulation result which is used to validate it.

If the error percentage is within the range of ±5%, it is considered acceptable [30]. Additionally, a variety of solar irradiation levels and a temperature of 25 °C are used to study the functioning of the PV module.

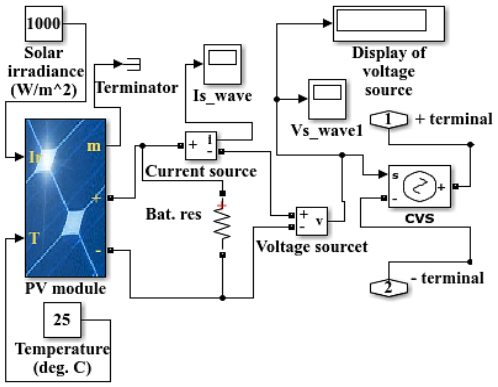

Figure 1. Modelling of PV module as DC voltage source

2.2. Proposed design of DC-DC buck converter based on the parameter tuning of PIDG controller

A DC-DC buck converter as shown in Figure 2 is designed to decrease the output voltage, V_{outpv} of 20.64 from PV module (as the input voltage of DC-DC buck converter) to be 14.7 V (as the output voltage of DC-DC buck converter, V_{out}). The MOSFET is as switching component that its gate terminal is driven by PWM generator with its duty cycle is D and its frequency, f is 10 kHz. The DC-DC buck converter is designed for the output power, P_{out} of 150 W. The duty cycle, D, inductor, L, capacitor, C, resistor, R (1) to (7), and the transfer function of DC-DC converter is given by (8) [17], [29].

$$D = \frac{V_{out}}{V_{in}} \tag{1}$$

The output current, I_{out}, the ripple of inductor current, ΔI_L and the ripple of output voltage, ΔV_{out} are calculated by (2) to (4).

$$I_{out} = \frac{P_{out}}{V_{out}} \tag{2}$$

$$\Delta I_L = 1\% \text{ x } I_{out} \tag{3}$$

$$\Delta V_{out} = 0.1\% \text{ x } V_{out} \tag{4}$$

$$L = \frac{V_{out}(V_{in}-V_{out})}{\Delta I_L f V_{in}} \tag{5}$$

$$C = \frac{\Delta I_L}{8 f \Delta V_{out}} \tag{6}$$

$$R = \frac{V_{out}}{I_{out}} \tag{7}$$

$$\frac{V_{out}(s)}{D(s)} = \frac{V_{in}}{LCS^2+\frac{L}{R}S+1} \tag{8}$$

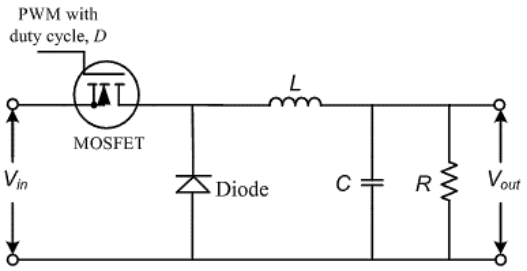

Figure 2. DC-DC buck converter

The DC-DC buck converter is as a plant that its output voltage is controlled by PIDG controller through out the PWM generator to the gate terminal of MOSFET. Figure 3 shows a proposed PIDG controller that it is PID controller connected by a gain, G in a series connection. The transfer function of PIDG controller is given by (9) by taking that K_p is multiplied by $e(t)$ $\{K_p \text{x} e(t)\}$, K_I is multiplied by $\int e(t)$ $\{K_I \text{x} \int e(t)\}$, and K_D is multiplied by $\frac{de(t)}{dt}$ $\left\{K_D \text{x} \frac{de(t)}{dt}\right\}$.

$$\frac{D(s)}{E(s)} = \frac{K_D S^2+K_P S+K_I}{S}.G \tag{9}$$

A block diagram of the plant (DC-DC buck converter), the PIDG controller with a feed back system is shown in Figure 4. The transfer function of DC-DC converter, PIDG controller is given by (10).

$$\frac{V_{out}(s)}{V_{ref}(s)} = \frac{(K_D S^2+K_P S+K_I).G.V_{in}}{\left(LCS^2+\frac{L}{R}S+1\right).S+(K_D S^2+K_P S+K_I).G.V_{in}} \tag{10}$$

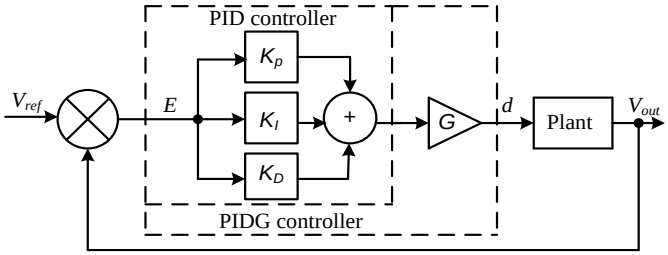

Figure 3. A proposed PID controller that it is connected by a gain, *G* and the plant in a series connection

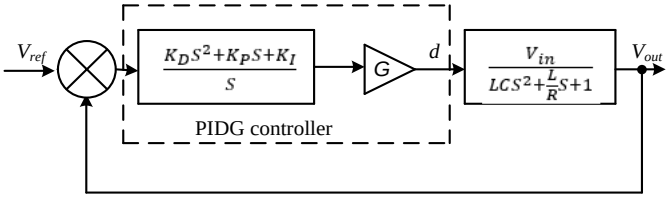

Figure 4. A block diagram of the plant (DC-DC buck converter) and the PIDG controller

The parameter tuning of PIDG controller (K_P, K_I, and K_D) is conducted by taking an equation as stated (11) and for G=1 as in (12), thus the values of K_P, K_I, and K_D are given by (13) to (15). The effect of gain, G on the settling time and the time to achieve the values of steady state are observed and analyzed on the performance of DC-DC buck converter.

$$(K_D S^2 + K_P S + K_I).G = LCS^2 + \frac{L}{R}S + 1 \quad (11)$$

$$K_D S^2 + K_P S + K_I = LCS^2 + \frac{L}{R}S + 1 \quad (12)$$

$$K_D = LC \quad (13)$$

$$K_P = \frac{L}{R} \quad (14)$$

$$K_I = 1 \quad (15)$$

2.3. Implementation of PIDG controller on the maximum photovoltaic power point for battery charging system using Simulink MATLAB

Figure 5 shows the implementation of PIDG controller on the maximum photovoltaic power point (MPVPP) for battery charging system using Simulink MATLAB. The DC-DC buck converter is created Figure 2 with its parameters (duty cycle (*D)*, inductor (*L)*, capacitor (C), and resistor (*R)* following) are calculated and they are filled into each block parameter in Simulink MATLAB (1) to (7). The DC-DC buck converter is as MPVPP device that is applied to charge 12 V battery.

The PV module operates if it obtains the solar irradiance with a certain temperature value. In this case, the temperature of 25 °C and solar irradiance of 1000 W/m^2 are tested to the PV module, thus it is obtained a required output voltage and it is as the input voltage of DC-DC buck converter, thus its output voltage of 14.7 V and its output power of 150 W are obtained. The output terminal of DC-DC buck converter is connected to 12 V battery with its specification is shown in Table 2. The performance of PV module, DC-DC buck converter and battery are observed and analyzed.

The gain, *G* that it is in the PIDG controller as shown in Figure 5 is observed. The observation is based on its required changing to know its effect of the performance of DC-DC buck converter by varying the gain, G in the DC-DC buck converter and PIDG controller. The gain, *G* takes an important action in the overall controller system, specially in the settling time and the time to achieve the steady state values of performance of DC-DC buck converter, also it plays a role in speeding up the battery charging process or in speeding up the state of charge (SOC) of battery.

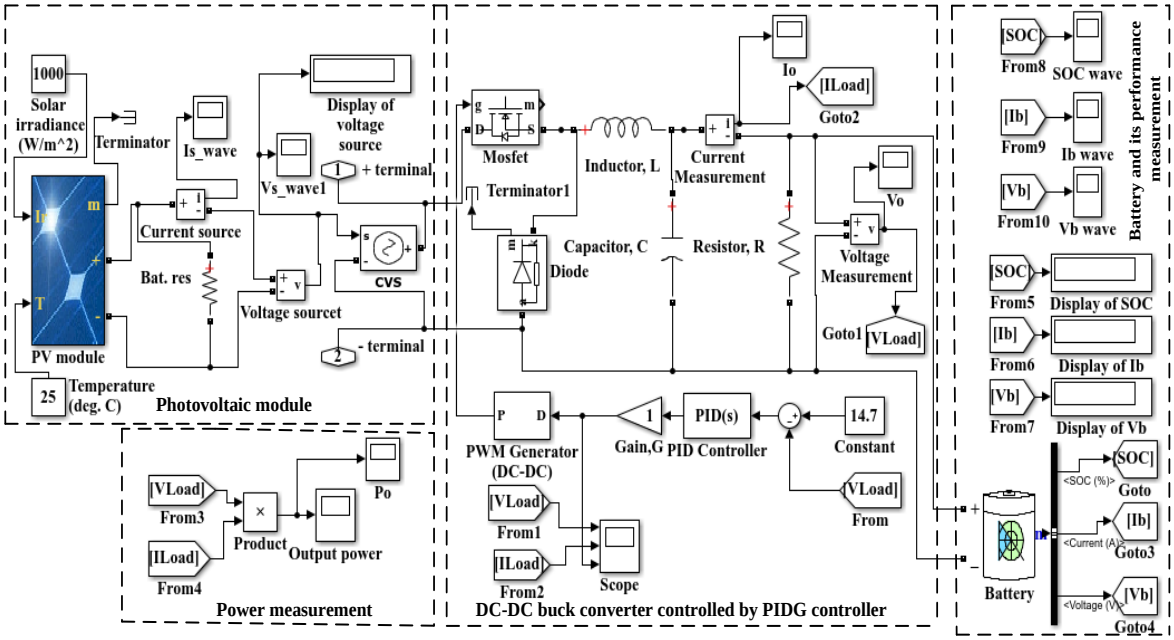

Figure 5. Implementation of PIDG controller on the MPVPP for battery charging system using MATLAB

Table 2. Battery specification

Parameters	Value
Maximum capacity	7.3 Ah
Fully charge voltage	13.07 V
Nominal discharge current	1.4 A
Internal resistance	0.0171 Ω
Capacity at nominal voltage	2.171 Ah

3. RESULTS AND DISCUSSION

This section displays and analyzes the results of the simulations of the PV module performance, the DC-DC buck converter performance, and the battery performance. The simulations of the PV module performance (short circuit current, open circuit voltage, and maximum power) are verified using the electrical parameters from the PV module data sheet, the DC-DC buck converter performance is simulated using its input voltage, output current, output voltage, and output power, and the battery performance is simulated using its input voltage, current, and SOC.

3.1. Photovoltaic module performance and its validation

In this part, the electrical properties from the PV module's data sheet under STC conditions are validated against the simulation findings. It is predicated on the power-voltage curve and current-voltage curve simulation findings, which are displayed in Figures 6(a) and (b), respectively. Table 3 displays the maximum power, open circuit voltage, and short circuit current based on the data sheet and simulation results (see Table 1). To ensure that the simulation findings are appropriate and applicable to the MPVPP for battery charging system, they are checked using the error percentage.

The simulation findings are validated using the PV module's three electrical parameters (maximum power, open circuit voltage, and short circuit current). Table 3 demonstrates that there is no difference in the error percentage between the simulation result in Figure 6(a) and the data sheet of short circuit current, indicating that there is no difference between the both. Additionally, there is no difference between the simulation result and the open circuit voltage data sheet, as shown by the 0% error percentage between the simulation result and the data sheet in Figure 6(a). Although the data sheet of maximum power and the simulation result in Figure 6(b) have an error percentage of -3.3%, this still means that the error percentage is within the permitted range of ±5%. The simulation result's value is less than the data sheet's value, as indicated by the negative sign.

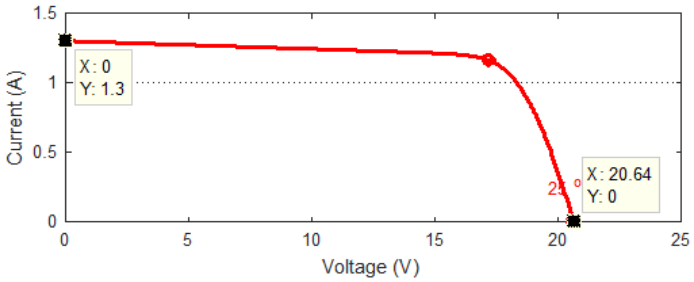

(a)

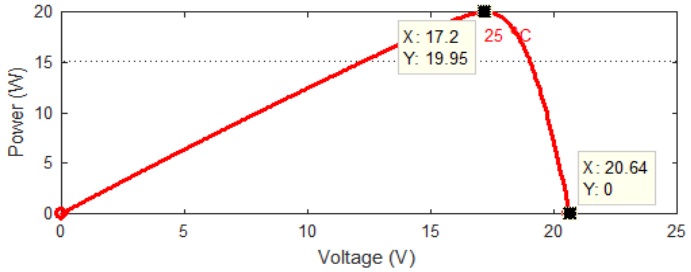

(b)

Figure 6. The performance of PV module: (a) current-voltage curve and (b) power-voltage curve

Table 3. Comparison of simulation results and data sheet of PV module

Parameters	Simulation result	Data sheet	Error percentage (%)
Short circuit current	1.3 A	1.3 A	0
Open circuit voltage	20.64 V	20.64 V	0
Maximum power	19.95 W	20 W	-3.3

3.2. Performance DC-DC buck converter

Two circumstances are used to observe the DC-DC buck converter's performance: STC conditions and different solar irradiation levels. This section examines and evaluates the DC-DC buck converter's input voltage, output voltage, output current, and output power in both scenarios. Additionally, the impact of the PID controller's gain, *G*, on the DC-DC buck converter's performance is noted and examined.

3.2.1. Performance DC-DC buck converter under STC condition and variuos solar irradiance

Figure 7(a) shows the voltage of PV module, it has a transient condition at the initial time, it is around 61.95 V or around 42.07 V from its steady state value. The transient condition is due to the release of stored energy by PV module when connected to the DC-DC buck converter. The transient condition is until the time of 0.0137 s and after that a steady state of PV module voltage is reached, it is 19.88 V. The voltage of PV module is as the input voltage of DC-DC buck converter to operate it and the battery charging system.

Figure 7(b) shows the output voltage of the DC-DC buck converter. The DC-DC buck converter is designed for the output voltage of 14.7 V. Based on Figure 7(b), the output voltage of DC-DC buck converter is 14.7 V, it is similar to its voltage design (its error percentage is 0%) and it indicates that there is no different between the output voltage designed and simulation. Also, it indicates that the simulation result of the output voltage can be accepted to be applied for charging a 12 V battery.

When the output voltage and the output power designed are 14.7 V and 150 W, respectively, thus the output current is 10.2 A. It is similar to the simulation result of output current of 10.2 A as shown in Figure 7(c). Figure 7(d) shows the output power of the DC-DC buck converter. The DC-DC buck converter is designed for the output power of 150 W. Based on Figure 7(d), the output power of DC-DC buck converter is 150 W, its error percentage is 0%. It indicates that the simulation result is same with the output power designed and it is acceptable to be applied to charge the battery. Thus, based on Figure 7, (5) to (7) and (13) to (15), the electrical parameter results of DC-DC converter are shown in Table 4.

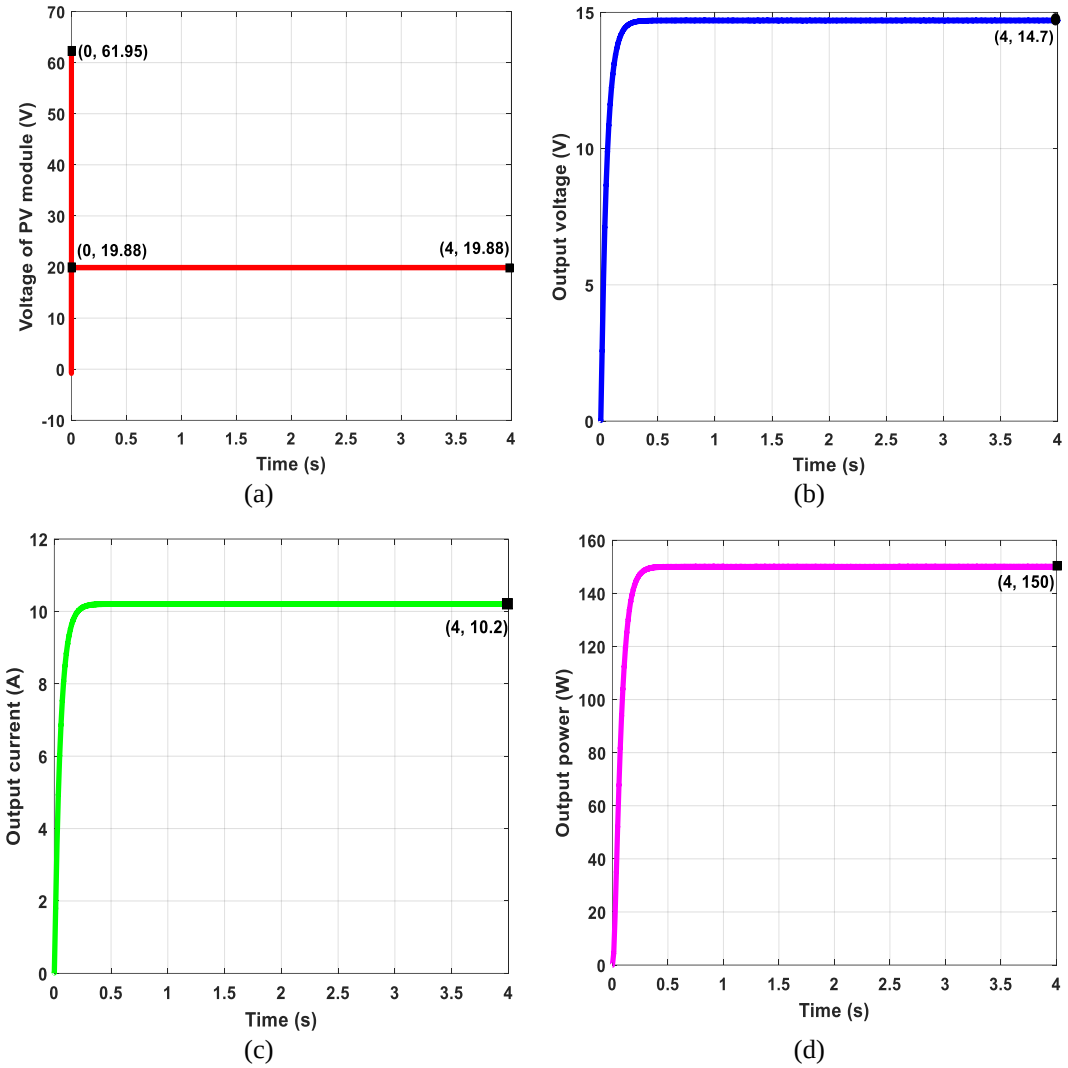

Figure 7. The performance of PV module and DC-DC buck converter: (a) voltage of PV module, (b) output voltage of DC-DC buck converter, (c) output current of DC-DC buck converter, and (d) output power of DC-DC buck converter

Table 4. The electrical parameters of DC-DC buck converter

Parameters	Value
Inductor, *L*	0.0046 H
Capacitor, *C*	86.77 µF
Resistor, *R*	1.44 Ω
Proportional, K_P	0.0032
Integral, K_I	1
Derivative, K_D	4×10^{-7}
Input voltage, *Vin*	19.88 V
Output voltage, *Vout*	14.7 V
Output current, *Iout*	10.20 A
Output power, *Pout*	149.9 W

Figure 8 shows the output voltage and power of the DC-DC buck converter for changing of solar irradiance from 1000 W/m^2 to be 300 W/m^2 at the time of 2 seconds. The changing of solar irradiance does not affect the performance of DC-DC buck converter significantly. The performances of DC-DC buck converter are affected at the time of solar irradiance changed, in this condition, a transient condition occurs with a lower value, but can be stable to their steady state values, it is due to that the PIDG controller can control the PWM signal to drive MOSFET in the circuit of DC-DC buck converter.

Figures 8(a) and (b) show the output voltage and power of DC-DC buck converter before and after occurring the changing of solar irradiance. The output voltage and power are 14.7 V and 150 W before the decreasing of solar irradiance, respectively. When the solar irradiance decreases to be 300 W/m^2 at the time of 2 seconds, thus the output voltage and power decrease to be 12.94 V and 115.3 W, respectively. But this condition can be stable back by PIDG controller, thus again the output voltage and power to be 14.7 V and 150 W, respectively after the decreasing of solar irradiance.

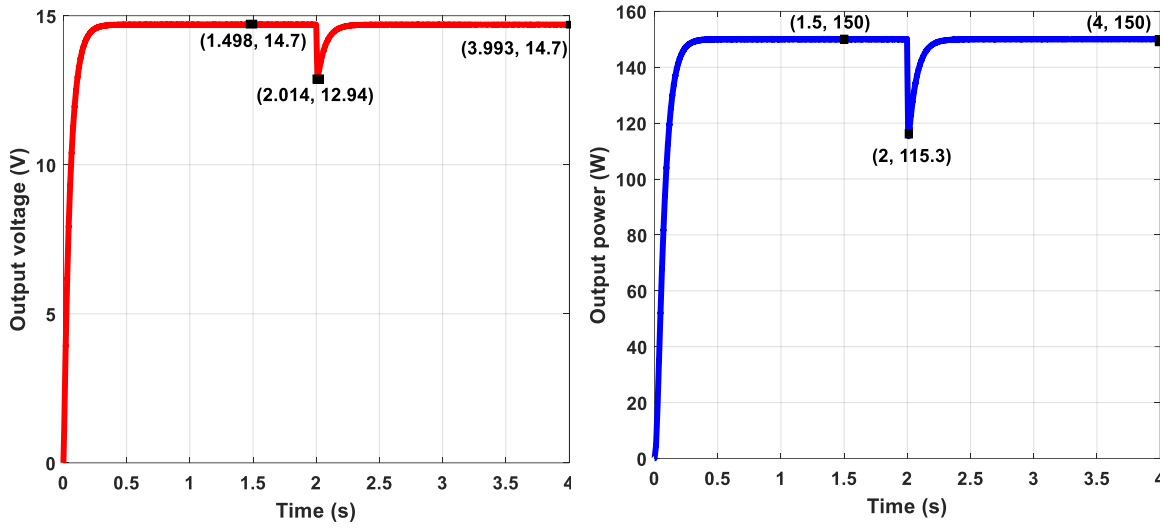

(a) (b)

Figure 8. The performance of DC-DC buck converter for changing of solar irradiance of 1000 W/m^2 to be 300 W/m^2: (a) output voltage and (b) output power

3.2.2. Effect of gain, *G* on the performance of DC-DC buck converter

The gain, G is a multiplication factor of parameters (K_P, K_I, and K_D) on PIDG controller as shown by (11). It is due to the parameters are constant as shown by (13) to (15), thus the multiplication results between each parameter and the gain, G is directly proportional to the gain. If the gain, G is higher, thus the multiplication result is also higher. In this case, the multiplication result of each parameter does not act to control the PWM signal to drive the gate terminal of MOSFET, but it is a submission result of the overall multiplication result of each parameter.

Figure 9 shows the effect of gain, G on the performance of DC-DC buck converter, it is only shown the output voltage for analyzes. It is tested for the gain, G=1, 2, 3, and 4 and they give significant effect on the time to reach their steady state value of output voltage. The output voltage of 14.7 V is remained in steady condition for the different value of gain, G. Only the time to reach the steady state is affected, if the gain, G is higher, thus the time to reach the steady state is shorter. It indicates a higher gain, G is better to be given in the PIDG controller to achieve the shortest settling time and the time to reach its steady state value of output voltage of DC-DC buck converter.

Figure 10 shows the settling time of the output voltage of DC-DC buck converter. It is plotted as a graph of the settling time versus gain, G. The gain, G is varied for the value of 2 to 20 with the range of 2. The gain, G gives a significant effect on the settling time of the performance of DC-DC buck converter. The graph shows that the higher gain, G, the shorter settling time of output voltage of DC-DC buck converter.

Table 5 shows settling time comparison without and with gain, G=10. This comparison condition for the solar irradiance of 1000 W/m^2, 800 W/m^2, 600 W/m^2, 400 W/m^2, and 300 W/m^2. Each solar irradiance applied in the MPVPP system shows that the gain, G gives a significant effect on the its settling time of the output voltage of DC-DC buck converter. The higher solar irradiance, the lower settling time for both without and with gain, G, but with gain, G has lower settled time than without gain, G for the same solar irradiance. An improvement of settling time obtained for the MPVPP system with gain, G, it contributes an improvement of 89.6% for each solar irradiance applied in the MPVPP system.

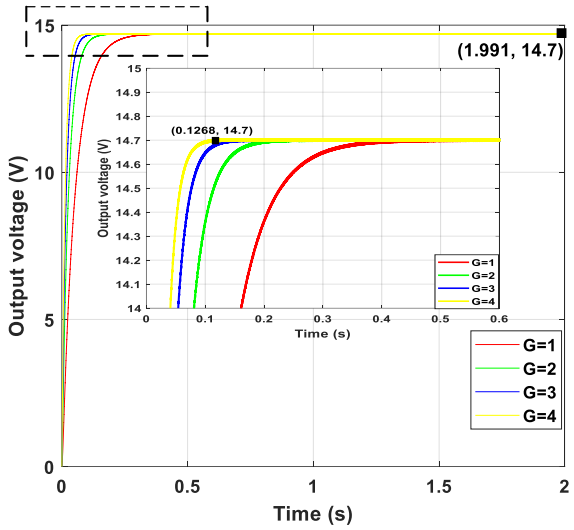

Figure 9. Effect of gain, *G* on the output voltage of DC-DC buck converter

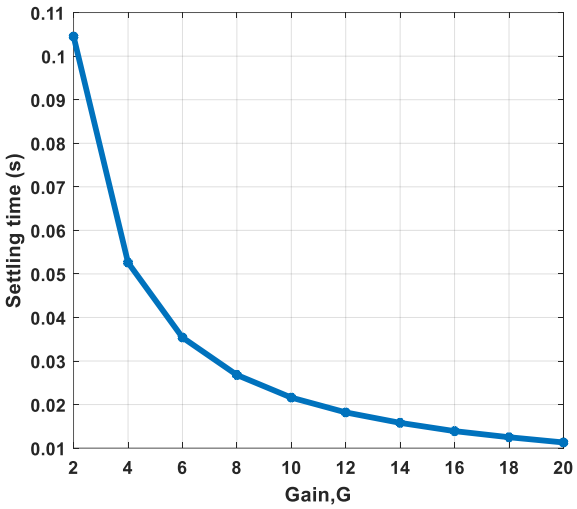

Figure 10. Settling time versus gain, *G* for the output voltage of DC-DC buck converter

Table 5. Settling time comparison without and with gain, *G*=10

Solar irradiance (W/m^2)	Settling time (second)		Improvement percentage (%)
	Without gain, *G*	With gain, *G*	
1000	0.2083	0.0216	89.6
800	0.2106	0.0219	89.6
600	0.2143	0.0222	89.6
400	0.2229	0.0231	89.6
300	0.2438	0.0252	89.6

3.3. Battery performance

The battery performance is observed for the PV module operation with solar irradiance of 1000 W/m^2 and the temperature of 25 °C and for the gain *G*=20 on the PID controller. The main objective of giving a value of gain, *G*=20 is to obtain the shortest time to reach the steady state condition of DC-DC buck converter, thus it gives a good battery performance as shown in Figure 11. The battery performance observed are the battery voltage, battery current and SOC.

Figure 11(a) shows the output voltage of DC-DC buck converter, it is as the battery voltage as shown in Figure 11(b). The battery voltage occurs a transient voltage of 15.07 V at the initial time, a small oscillation occurs and it can be controlled by PIDG controller to reach its steady state voltage of 14.7 V. The battery voltage of 14.7 V is always in stable condition during the charging process. The battery current is -26.51 A during the charging process as shown in Figure 11(c). The negative sign indicates that the battery in the charging process.

The SOC of 12 V, 7 Ah battery is 25% of fully charging condition in the charging initial time. The SOC can reach 30.43% of fully charging condition for the charging process time of 4 seconds as shown in Figure 11(d). The increasing of SOC is 5.43% for 4 seconds or the percentage of SOC needed in 1 second is 1.36%. The SOC of battery needs 75% to reach its fully charging condition. Thus, the time needed by battery to reach its fully charging condition is around 55 seconds.

The output voltage of DC-DC buck converter occurs an oscillation at the early time when it is connected to the battery and before reaching its steady state value of 14.7 V (refer Figures 11(a) and (b)). A detail observation of output voltage oscillation is shown in Figure 12 for the time of 0.28 s to 0.5 s with various gain, *G*. The time is chosen because it is near the time of its steady state value, and the main objective of observation is to analyze the effect of gain, *G* on its oscillation or stability in term of its oscillation peak and settling time value. It can be stated that the all gain, *G* applied on the MPVPP system always generate a stable system, it means each gain, *G* reaches its steady state value of 14.7 V. It only affects the oscillation peak and settling time value of output voltage. The higher gain, *G* generates the higher oscillation peak, but the shorter settling time and the shorter time to reach its steady state value. Based on the time to reach its steady state, it can be stated that the higher gain, *G* generates a more stable system.

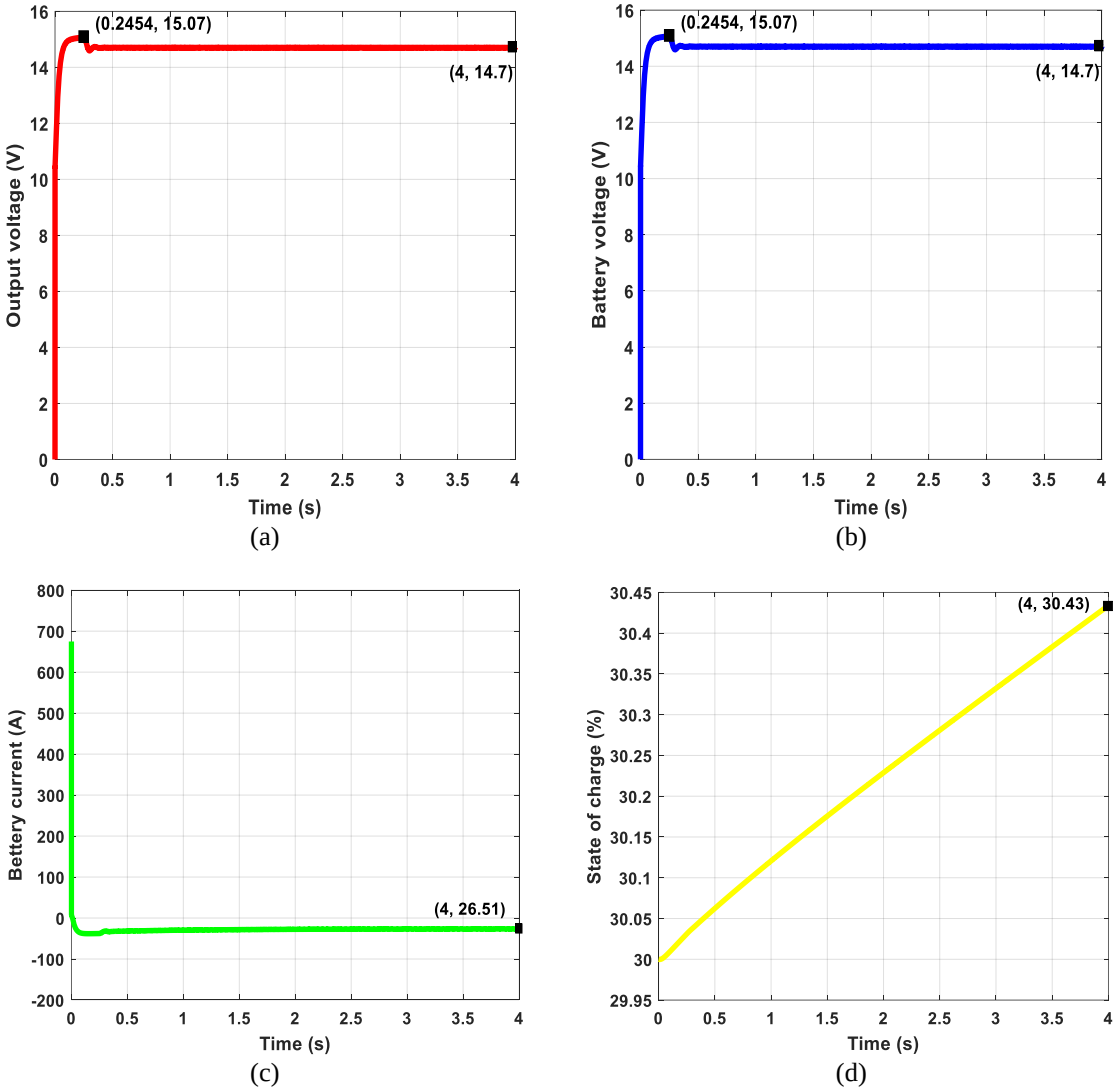

Figure 11. Battery performance: (a) output voltage of DC-DC buck converter, (b) battery voltage, (c) battery current, and (d) SOC

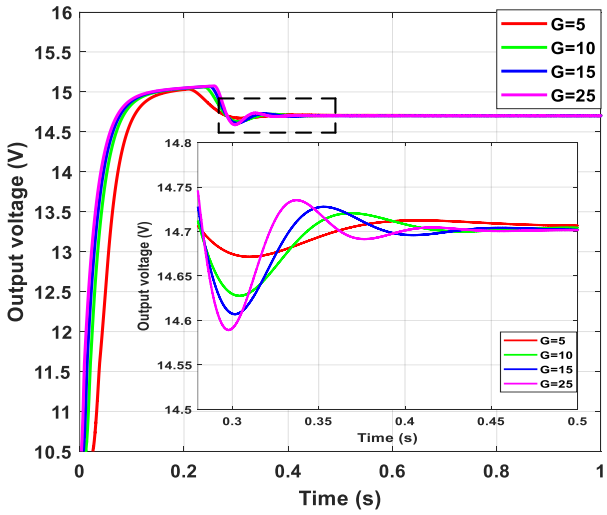

Figure 12. Oscillation of output voltage on the DC-DC buck converter for various gain, *G*

4. CONCLUSION

A DC-DC buck converter is designed for its input voltage, output voltage and power are 20.64 V, 14.7 V, and 150 W, respectively. The input voltage of DC-DC buck converter is supplied by PV module and Its output is connected to 12 V, 7 Ah battery. The switching component of DC-DC buck converter is driven by PMW signal that it is controlled by PIDG controller with required values of parameters (proportional, K_P, integral, *KI*, and derivative, K_D) and gain, *G*. Some conclusions can be given as stated below.

The electrical parameters of inductor (L) of 0.0046 H, capacitor (C) of 86.77 µF and resistor (R) of 1.44 Ω are required to achieve the proposed design of DC-DC buck converter. A PIDG controller with its parameters of proportional, K_P=0.0032, integral, K_I=1, and derivative, K_D=4×10^{-7} are suitable to control the PWM signal that it drives the switching component of DC-DC buck converter. For this condition, the output voltage of 14.7 V can be remained throughout the operation of DC-DC buck converter.

The effect of gain, *G* on the performance of DC-DC buck converter is also observed and analyzed. It gives significant effect on the time to reach their steady state value of output voltage. The output voltage of 14.7 V is remained in steady condition for the different value of gain, *G*. Only the time to reach the steady state is affected, if the gain, *G* is higher, thus the time to reach the steady state is shorter. It indicates a higher gain, *G* is better to be given in the PIDG controller to achieve the shortest settling time and the shortest time to reach its steady state value of output voltage of DC-DC buck converter.

The DC-DC buck converter is applied to charge 12 V, 7 Ah battery. The initial condition of battery SOC is 25%, it can increase to be 30.43% for charging in the time of 4 seconds. If the battery needs 75% to reach its full charging condition. Thus, it needs arround 55 seconds to reach the fully charging condition.

ACKNOWLEDGMENTS

Thank you very much for the Fundamental Research-Regular grant with the award number 122/C3/DT.05.00/PL/2025 from the Ministry of Education, Culture, Research and Technology of Indonesia. Also, thank you very much for Universiti Malaysia Perlis (UniMAP), especially for Center of Excellence for Renewable Energy (CERE) that has a good collaboration with Universitas Prima Indonesia (UNPRI).

FUNDING INFORMATION

The Ministry of Education, Culture, Research and Technology of Indonesia throughout the Fundamental Research-Regular grant with the award number 122/C3/DT.05.00/PL/2025 is a source of funding agency.

AUTHOR CONTRIBUTIONS STATEMENT

This journal uses the Contributor Roles Taxonomy (CRediT) to recognize individual author contributions, reduce authorship disputes, and facilitate collaboration.

Name of Author	C	M	So	Va	Fo	I	R	D	O	E	Vi	Su	P	Fu
Muhammad Irwanto	✓	✓	✓		✓	✓		✓	✓	✓				
Togar Timoteus Gultom		✓				✓		✓	✓	✓				
Habib Satria	✓		✓					✓	✓	✓				
Baharuddin Ismail		✓				✓		✓	✓	✓				
Christin Erniati Panjaitan					✓					✓			✓	
Mahdi Syukri	✓		✓	✓			✓			✓				

C : **C**onceptualization
M : **M**ethodology
So : **So**ftware
Va : **Va**lidation
Fo : **Fo**rmal analysis
I : **I**nvestigation
R : **R**esources
D : **D**ata Curation
O : Writing - **O**riginal Draft
E : Writing - Review & **E**diting
Vi : **Vi**sualization
Su : **Su**pervision
P : **P**roject administration
Fu : **Fu**nding acquisition

CONFLICT OF INTEREST STATEMENT

Authors state no conflict of interest.

DATA AVAILABILITY

The data of electrical parameter of photovoltaic module as stated in Table 1 that support the findings of this study are openly available in Journal of Physics: Conference Series, vol.1529, no. 042096, pp. 1-10, 2020, doi: 10.1088/1742-6596/1529/4/042096, reference number [30].

REFERENCES

[1] S. M. Heidari and A. Anctil, "Material Requirement and Resource Availability for Silicon Photovoltaic Laminate Manufacturing in the Next 10 Years," *Proceedings of the 2021 IEEE 48th Photovoltaic Specialists Conference (PVSC)*, 2021, pp. 1768–1772, doi: 10.1109/PVSC43889.2021.9518663.

[2] M. Tao, H. Hamada, T. Druffel, J. J. Lee, and K. Rajeshwar, "Review—Research Needs for Photovoltaics in the 21st Century," *ECS Journal of Solid State Science and Technology*, vol. 9, 2020, doi: 10.1149/2162-8777/abd377.

[3] Z. Li, C. Tang, C. Liu, and Y. Chen, "Integrated Control Technology of Photovoltaic Reactive Power with Source Network Coordination Based on Multi-Agent Technology," in *IOP Conference Series: Earth and Environmental Science*, 2021, vol. 714, doi: 10.1088/1755-1315/714/4/042006.

[4] A. A. Kareim, "Simulation and Comparison of Modeling of Photovoltaic Modules During Different Values of Solar Irradiations Whilst Temperature of Twenty Five Degree Celsius," in *IOP Conference Series: Materials Science and Engineering*, 2020, vol. 928, doi: 10.1088/1757-899X/928/2/022112.

[5] I. Mathews *et al.*, "Analysis of CdTe Photovoltaic Cells for Ambient Light Energy Harvesting," *Journal of Physics D: Applied Physics*, vol. 53, 2020, doi: 10.1088/1361-6463/ab94e6.

[6] O. Slimani, M. Mebrouki, and H. Sebbagh, "Techno-Economic Analysis of a Stand-Alone Photovoltaic System with Different Tilt Angle," *Proceedings of the 2024 International Conference on Advances in Electrical and Communication Technologies (ICAECOT)*, 2024, pp. 1-6, doi: 10.1109/ICAECOT62402.2024.10828914.

[7] L. Zaghba, M. K. Benbitour, A. Fezzani, A. Borni, and A. Bouchakour, "Detailed Simulation Analysis of Rooftop Stand-Alone Photovoltaic Systems Installed in Arid Regions of Algeria," *Proceedings of the 2024 IEEE International Multi-Conference on Smart Systems & Green Process (IMC-SSGP)*, 2024, pp. 1-6, doi: 10.1109/IMC-SSGP63352.2024.10919863.

[8] J. Zhu, J. Qiang, C. Feng, and D. He, "Design of Sliding Mode Adaptive DC–DC Converter Based on Function Approximation," in *Journal of Physics: Conference Series*, 2021, vol. 2005, doi: 10.1088/1742-6596/2005/1/012109.

[9] I. Alhurayyis, A. Elkhateb, and J. Morrow, "Isolated and Nonisolated DC-to-DC Converters for Medium-Voltage DC Networks: A Review," *IEEE Journal of Emerging and Selected Topics in Power Electronics*, vol. 9, no. 6, pp. 7486–7500, 2021, doi: 10.1109/JESTPE.2020.3028057.

[10] A. Sweatha, B. Baskaran, and P. Duraipandy, "An Extensive Review of DC–DC Converter Topologies for Water-Pumping Application," *Proceedings of the 2022 International Conference on Innovations in Science and Technology for Sustainable Development (ICISTSD)*, 2022, pp. 151-156, doi: 10.1109/ICISTSD55159.2022.10010591.

[11] Y. Li, "A Comparison of FLC MPPT Techniques and HC MPPT Techniques for Photovoltaic Systems," in *Journal of Physics: Conference Series*, 2023, vol. 2634, doi: 10.1088/1742-6596/2634/1/012015.

[12] M. Situmorang and B. Peranginangin, "Performance Assessment of Photovoltaic Generator Power System Using Maximum Power Point Tracking (MPPT) DC to DC Boost Converter and DC to AC Inverter," in *IOP Conference Series: Journal of Physics: Conference Series*, 2020, vol. 1485, doi: 10.1088/1742-6596/1485/1/012061.

[13] F. Zishan, A. Barmakh, and O. D. D. Montoya-Giraldo, "A Non-Isolated Synchronous Buck DC-DC Converter, ZVS Topology Under CCM and DCM Conditions," *Results in Engineering*, vol. 23, pp. 1-20, 2024, doi: 10.1016/j.rineng.2024.102440.

[14] R. Uthirasamy, J. Karpagam, U. Subramaniam, and V. J. Vijayalakshmi, "Extended Boost DC–DC–AC Converter for Electric Vehicle Applications," in *IOP Conference Series: Materials Science and Engineering*, 2020, vol. 937, doi: 10.1088/1757-899X/937/1/012045.

[15] S. Danyali, A. Moradkhani, O. A. Abdaumran, M. Shirkhani, and Z. Dadvand, "A Novel Multi-Input Medium-Gain DC-DC Boost Converter With Soft-Switching Performance," *International Journal of Electrical Power and Energy Systems*, vol. 155, 2024, doi: 10.1016/j.ijepes.2023.109629.

[16] V. H. García-Rodríguezа, R. C. Ambrosio-Lázaro, J. H. Pérez-Cruzc, S. T. Tavera-Mosquedad, and C. R. Ascencio-Hurtado, "Bipolar Voltage Tracking Control for DC/DC Boost Converter–Full-Bridge Buck Inverter System: Design and Analysis," *Results in Engineering*, vol. 25, pp. 1-10, 2025, doi: 10.1016/j.rineng.2024.103690.

[17] X. Xu, Y. Zhu, F. Wu, X. Chen, and C. Y. Su, "Bumpless Transfer Control for DC-DC Buck-Boost Converter Modeled by Switched Affine Systems," *Control Engineering Practice*, vol. 159, pp. 1-8, 2025, doi: 10.1016/j.conengprac.2025.106320.

[18] M. Morey, M. Golla, M. M. Garg, N. Gupta, and A. Kumar, "A High Gain Z-Source Boost DC–DC Converter With Common Ground for Solar PV Applications," *Electric Power Systems Research*, vol. 232, pp. 1-15, 2024, doi: 10.1016/j.epsr.2024.110405.

[19] R. Rajesh and S. N. Deepa, "Design of Direct MRAC Augmented With 2 DoF PIDD Controller: An Application to Speed Control of a Servo Plant," *Journal of King Saud University – Engineering Sciences*, vol. 32, pp. 310–320, 2020, doi: 10.1016/j.jksues.2019.02.005.

[20] M. Gengaraj, L. Kalaivani, and R. Rajesh, "Investigation on Torque Sharing Function for Torque Ripple Minimization of Switched Reluctance Motor: A Flower Pollination Algorithm Based Approach," *IETE Journal of Research*, vol. 69, no. 6, pp. 3678–3692, 2023, doi: 10.1080/03772063.2022.2112312.

[21] R. Rajesh and S. N. Deepa, "Design of State Feedback LQR Based Dual Mode Fractional-Order PID Controller Using Inertia Weighted PSO Algorithm: For Control of an Underactuated System," *Journal of The Institution of Engineers (India): Series C*, vol. 102, no. 6, pp. 1403–1417, 2021, doi: 10.1007/s40032-021-00756-x.

[22] R. Rajesh, "Optimal Tuning of FOPID Controller Based on PSO Algorithm With Reference Model for a Single Conical Tank System," *SN Applied Sciences*, 2019, vol. 1, doi: 10.1007/s42452-019-0754-3.

[23] M. E. Girgis and N. A. Elkhateeb, "Enhancing Photovoltaic MPPT With P&O Algorithm Performance Based on Adaptive PID Control Using Exponential Forgetting Recursive Least Squares Method," *Renewable Energy*, vol. 237, pp. 1-12, 2024, doi: 10.1016/j.renene.2024.121801.

[24] A. I. S. Ali and H. R. A. Mohamed, "Improved P&O MPPT Algorithm With Efficient Open-Circuit Voltage Estimation for Two-Stage Grid-Integrated PV System Under Realistic Solar Radiation," *International Journal of Electrical Power and Energy Systems*, vol. 137, pp. 1-12, 2022, doi: 10.1016/j.ijepes.2021.107805.

[25] A. Zhao, R. Zhu, and G. Wang, "Optimization and Comparison of Photovoltaic MPPT," in *Journal of Physics: Conference Series*, 2020, vol. 1626, doi: 10.1088/1742-6596/1626/1/012004.
[26] F. A. Eshete, D. P. Samajdar, and A. Kumar, "Implementation of Modified P&O and An Adaptive Fuzzy Logic Controller Based MPPT Tracking System Under Partial Shading and Variable Environmental Conditions," *Physica Scripta*, vol. 19, pp. 1-27, 2024, doi: 10.1088/1402-4896/ad3ff2.
[27] H. Wang, P. Ma, G. Hu, H. Wang, and Y. Zhou, "A Modified P&O Maximum Power Tracking Control Algorithm for Independent Wind Energy Conversion System," *Journal of Physics: Conference Series*, vol. 2917, pp. 1-9, 2024, doi: 10.1088/1742-6596/2917/1/012027.
[28] J. Ouyang, J. Wu, and M. Lin, "Controller Design of a Novel Interleaved Parallel Bi-Directional DC–DC Converter," in *Journal of Physics: Conference Series*, vol. 2731, 2024, doi: 10.1088/1742-6596/2731/1/012018.
[29] A. S. Samosir, T. Sutikno, and L. Mardiyah, "Simple Formula for Designing the PID Controller of a DC–DC Buck Converter," *International Journal of Power Electronics and Drive Systems*, vol. 14, no. 1, pp. 327–336, 2023, doi: 10.11591/ijpeds.v14.i1.pp327-336.
[30] M. Irwanto, N. Gomesh, B. Ismail, H. Alam, M. Masri, and B. S. Kusuma, "Performance of Nine-Level Transformerless Photovoltaic Powered Inverter (TPVPI) Using Technique of Equal Maximum Phase Delay Time," *Journal of Physics: Conference Series*, vol. 1529, 2020, doi: 10.1088/1742-6596/1529/4/042096.

BIOGRAPHIES OF AUTHORS

Muhammad Irwanto received his Ph.D. degree in Electrical System Engineering from Universiti Malaysia Perlis (UniMAP), Malaysia in 2012. He is currently a researcher in the Center of Excellence for Health Based on IoT and Renewable Energy, Department of Electrical Engineering, Faculty of Science and Technology, Universitas Prima Indonesia (UNPRI). He is also fellow of Centre of Excelence for Renewable Energy (CERE), Faculty of Electrical Engineering and Technology, Universiti Malaysia Perlis (UniMAP). His research interest includes power electronic, electrical power system stability, solar energy, and photovoltaic application system. He can be contacted at email: muhammadirwanto@unprimdn.ac.id or irwanto@unimap.edu.my.

Togar Timoteus Gultom received his Master degree in Electrical Engineering, from Institut Sains and Teknologi Nasional, Jakarta, Indonesia. He is a lecturer at the Department of Electrical Engineering, Faculty of Science and Technology, Universitas Prima Indonesia (UNPRI). He is very active in the activity in area of biomedical engineering, especially for repairing the device of biomedical. His research interest includes power system analysis, electrical machines, and transformer. He can be contacted at email: togartimoteusgultom@unprimdn.ac.id.

Habib Satria received his Master degree in Electrical Engineering from Universitas Andalas, Indonesia, in 2018 He is currently a lecture in Department of Electrical Engineering, Universitas Medan Area, Indonesia. His research interests are new and renewable energy, concerning about solar power plant, automatic control system, IoT, real-time simulation, green computing, pattern recognition, and power system. He is a member of the International Association of Engineers (IAENG) and The Institution of Engineers Indonesia. He can be contacted at email: habib.satria@staff.uma.ac.id.

Baharuddin Ismail received his Ph.D. degree in Electrical System Engineering from Universiti Malaysia Perlis (UniMAP), Malaysia in 2015. He is currently a lecturer in Faculty of Electrical Engineering and Technology, Universiti Malaysia Perlis (UniMAP). He is also fellow of Centre of Excellence for Renewable Energy (CERE), Faculty of Electrical Engineering and Technology, Universiti Malaysia Perlis (UniMAP). His research interest includes power electronic and renewable energy system. He can be contacted at email: baha@unimap.edu.my.

Christin Erniati Panjaitan received S.T. degree in Telecommunication Engineering from Institut Teknologi Telkom (now: Telkom University) in 2010. She obtained M.Sc. in Electronic and Computer Engineering from National Taiwan University of Science and Technology (NTUST) in 2016. She is currently working as a lecturer of Electrical Engineering at Universitas Prima Indonesia. She is now pursuing Ph.D. in Biomedical Electronic Engineering at Universitas Malaysia Perlis (UniMAP). She can be contacted at email: christinpanjaitan@unprimdn.ac.id.

Mahdi Syukri received his Ph.D. degree in Electrical Engineering from Universitas Syiah Kuala (USK), Banda Aceh, Indonesia in 2024. He is currently a lecturer, Department of Electrical Engineering, Faculty of Technology Universitas Syiah Kuala (USK), Banda Aceh, Indonesia. His research interest includes power system, electrical power system stability, and electrical machines. He can be contacted at email: mahdisyukri@usk.ac.id.